145, 819 (1977).
8. T. F. Vogt, D. Solter, S. M. Tilghman, *Science* **236**, 301 (1987).
9. R. Godbout, R. S. Ingram, S. M. Tilghman, *Mol. Cell. Biol.* **6**, 477 (1986).
10. ———, *ibid.* **8**, 1169 (1988).
11. M. Guertin *et al.*, *ibid.*, p. 1398.
12. L. Muglia and L. B. Rothman-Denes, *Proc. Natl. Acad. Sci. U.S.A.* **83**, 7653 (1986).
13. K. Watanabe, A. Saito, T. Tamaoki, *J. Biol. Chem.* **262**, 4812 (1987).
14. S. G. Widen and J. Papaconstantinou, *Proc. Natl. Acad. Sci. U.S.A.* **83**, 8196 (1986).
15. R. E. Hammer, R. Krumlauf, S. A. Camper, R. L. Brinster, S. M. Tilghman, *Science* **235**, 53 (1987).
16. S. A. Camper and S. M. Tilghman, *Genes Dev.* **3**, 537 (1989).
17. M. Feuerman, R. Godbout, R. S. Ingram, S. M. Tilghman, *Mol. Cell. Biol.* **9**, 4204 (1989).
18. A. Tyner, R. Godbout, R. S. Compton, S. M. Tilghman, *J. Cell Biol.* **110**, 915 (1990).
19. A. Otsuru, S. Nagataki, T. Koji, T. Tamaoki, *Cancer* **62**, 1105 (1988).
20. A. M. Poliard *et al.*, *J. Cell Biol.* **103**, 777 (1986).
21. C. A. Pinkert, D. M. Ornitz, R. L. Brinster, R. D. Palmiter, *Genes Dev.* **1**, 268 (1987).
22. F. V. Chisari *et al.*, *Proc. Natl. Acad. Sci. U.S.A.* **84**, 6909 (1987).
23. J. Vacher and S. M. Tilghman, unpublished data.
24. A. D. Johnson and I. Herskowitz, *Cell* **42**, 237 (1985).
25. A. Winoto and D. Baltimore, *ibid.* **59**, 649 (1989).
26. P. Tripputi, S. L. Guerin, D. D. Moore, *Science* **241**, 1205 (1988).
27. B. D. Mariani, J. R. Lingappa, F. C. Kafatos, *Proc. Natl. Acad. Sci. U.S.A.* **85**, 3029 (1988).
28. H. J. Doyle, R. Kraut, M. Levine, *Genes Dev.* **3**, 1518 (1989).
29. R. W. Scott and S. M. Tilghman, *Mol. Cell. Biol.* **3**, 1295 (1983).
30. C. Auffray and F. Rougeon, *Eur. J. Biochem.* **107**, 303 (1980).
31. H. Aviv and P. Leder, *Proc. Natl. Acad. Sci. U.S.A.* **69**, 1408 (1972).
32. K. P. Dudov and R. P. Perry, *Cell* **37**, 457 (1984).
33. We thank R. Perry for the ribosomal protein gene probe and N. Mann for excellent help in the preparation of the manuscript. Supported by a grant from the NIH (CA44976). J.V. is on leave of absence from the Centre National de la Recherche Scientifique, Paris, France. S.M.T. is an Investigator of the Howard Hughes Medical Institute.

11 July 1990; accepted 11 September 1990

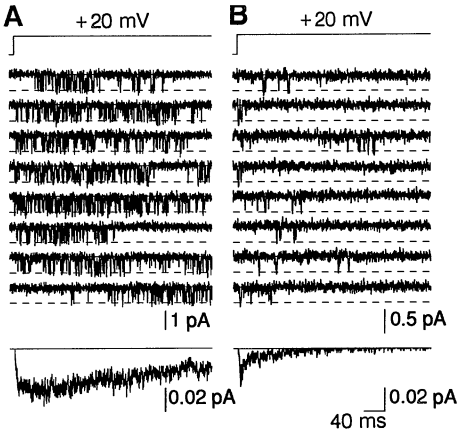

Fig. 1. Differences in single-channel gating with (**A**) Ba^{2+} and (**B**) Ca^{2+} as charge-carrier. (Top) Voltage protocol from holding potential of −50 mV. (Center) Representative traces from patches with a single Ca^{2+} channel. Unitary currents were low pass–filtered at (A) 2 kHz and (B) 0.8 kHz (*12*). (Bottom) Ensemble average of unitary current records. [(A) patch rle57; (B) patch r2es46.]

Calcium-Sensitive Inactivation in the Gating of Single Calcium Channels

DAVID T. YUE,* PETER H. BACKX, JOHN P. IMREDY

Voltage-activated calcium channels open and close, or gate, according to molecular transition rates that are regulated by transmembrane voltage and neurotransmitters. Here evidence for the control of gating by calcium was found in electrophysiological records of single, L-type calcium channels in heart cells. Conditional open probability analysis revealed that calcium entry during the opening of a single channel produces alterations in gating transition rates that evolve over the course of hundreds of milliseconds. Such alteration of calcium-channel gating by entry of a favored permeant ion provides a mechanism for the short-term modulation of single-ion channels.

CALCIUM CHANNELS FORM A VITAL link in the transduction of extracellular signals to numerous physiological processes, which include neurotransmitter release (*1*) and contraction (*2, 3*). To appreciate how Ca^{2+} channels function in this capacity, a rigorous understanding of their gating properties is necessary. Yet fundamental questions about Ca^{2+}-channel gating remain unanswered, in large part because of the complexities of Ca^{2+}-facilitated inactivation, a prominent feature of many Ca^{2+} channels whereby Ca^{2+} entry through the channel pore appears to speed inactivation (*4–7*). Conflicting viewpoints on this property arise from studies of macroscopic and single-channel Ca^{2+} currents. Macroscopic data hint that gating transition rates change slowly according to prior channel activity (*5*) and that elevations of intracellular Ca^{2+} concentrations ($[Ca^{2+}]_i$) predominate in modulating inactivation (*8*). In contrast, single-channel records have so far failed to reveal alterations in gating by bursts of Ca^{2+} entry (*9*) or by tonic elevations of $[Ca^{2+}]_i$ (*10*). These discrepancies leave open elementary questions about the very class of gating models and mechanisms required for Ca^{2+}-channel gating. This report aims to clarify some of these unresolved questions.

There are differences in the pattern of gating that result when Ba^{2+} substitutes for Ca^{2+} as the charge-carrier through L-type Ca^{2+} channels (Fig. 1) (*11*). With Ba^{2+}, the majority of records containing channel activity exhibit tightly clustered openings that often continue to the end of records (Fig. 1A). The ensemble average of the unitary Ba^{2+} currents declines very slowly, as expected without enhanced inactivation by Ca^{2+} ions (Fig. 1A, bottom). Although gating is similar when other permeant ions such as Sr^{2+} (*7, 12*) or Na^+ (*13*) are used in place of Ba^{2+}, a different picture emerges when Ca^{2+} carries the current: not only are unitary currents (*i*) smaller (−0.34 versus −0.85 pA), but openings occur less frequently and are rare by the end of each record (Fig. 1B). Accordingly, the ensemble average is smaller and declines faster (Fig. 1B, bottom). Although the overall nature of single-channel gating is unique with Ca^{2+} as the charge-carrier [but see (*14*)], these results could be explained by either of two schemes: Ca^{2+} entry could be producing slow changes in gating transition rates, as macroscopic studies (*5*) suggest; or the enhancement of inactivation might be occurring almost instantaneously with the passage of Ca^{2+} ions into the channel pore, consistent with prior single-channel reports (*9, 10*). The latter case would yield transition rates that appear to be invariant on the time scale of patch-clamp records.

To distinguish between these possibilities, we used conditional open probability analysis (COPA), developed by Sigworth (*15*) for macroscopic currents. Here single-channel records are used to calculate the conditional open probability $P_{oo}(t, t_j)$, defined as the chance that a channel is open at time t if it is known to be open at time t_j (*16*). Two properties of $P_{oo}(t, t_j)$ are relevant. (i) If rate constants remain constant ("homogeneous" process) and there is a single open state, then the decay of $P_{oo}(t, t_j)$ with increasing t ($t \geq t_j$) follows an invariant time course, independent of the choice of t_j (*17*). (ii) If Ca^{2+} entry progressively alters rate constants ("inhomogeneous" process), then the decay of $P_{oo}(t, t_j)$ should evolve with increasing t_j. Because a single open state predominates here (*16*), COPA can distinguish between homogeneous and inhomogeneous gating of the Ca^{2+} channel.

Department of Biomedical Engineering, The Johns Hopkins University School of Medicine, Baltimore, MD 21205.

*To whom correspondence should be addressed.

As a methodological check, COPA was performed when Ba^{2+} was the charge-carrier. Because there is little current-facilitated inactivation with Ba^{2+} (*6*, 7), gating rate constants should be invariant during a maintained voltage step. The simple open probability P_o is shown for orientation (Fig. 2A, trace 0). Traces 1 to 3 plot $P_{oo}(t, t_j)$ conditioned on time windows centered at t_j of 10, 50, and 170 ms (bars above P_o). The traces assume a value of unity at t_j (by definition) and subsequently decay to a slowly declining pedestal at ~0.1. The portion of traces preceding the peaks indicates the history of opening before time t_j. The important feature is that the decay of $P_{oo}(t, t_j)$ $(t > t_j)$ appears identical in all cases, as Fig. 2B confirms. After alignment at t_j, traces 1 to 3 superimpose (top) and difference traces (below) are flat. COPA therefore shows gating to be homogeneous when Ba^{2+} is the charge-carrier, supporting the validity of our analytical approach.

When Ca^{2+} supported the ion flux, we observed a very different result (Fig. 2C). The simple open probability (trace 0′) and identical conditioning-time windows (horizontal bars) are shown at top. In this case, the decay of $P_{oo}(t, t_j)$ from unity (traces 1′ to 3′) appears to change with t_j. This trend becomes obvious after time base expansion and alignment of traces at t_j (Fig. 2D). Comparison of the top set of traces indicates that the decay of $P_{oo}(t, t_j)$ becomes increasingly precipitous as t_j is delayed, as if a history of greater Ca^{2+} influx before t_j favors subsequent channel closure. The magnitude and consistency of this effect are demonstrated by the difference traces below, where the solid curve plots the mean from six patches. Thus, gating proceeds as an inhomogeneous process when Ca^{2+} carries charge; gating rate constants evolve slowly during a depolarization epoch.

An important question that remains is whether gating varies strictly as a function of prior openings, or trivially as a function of time spent at the activating step potential. Either of these explanations is consistent

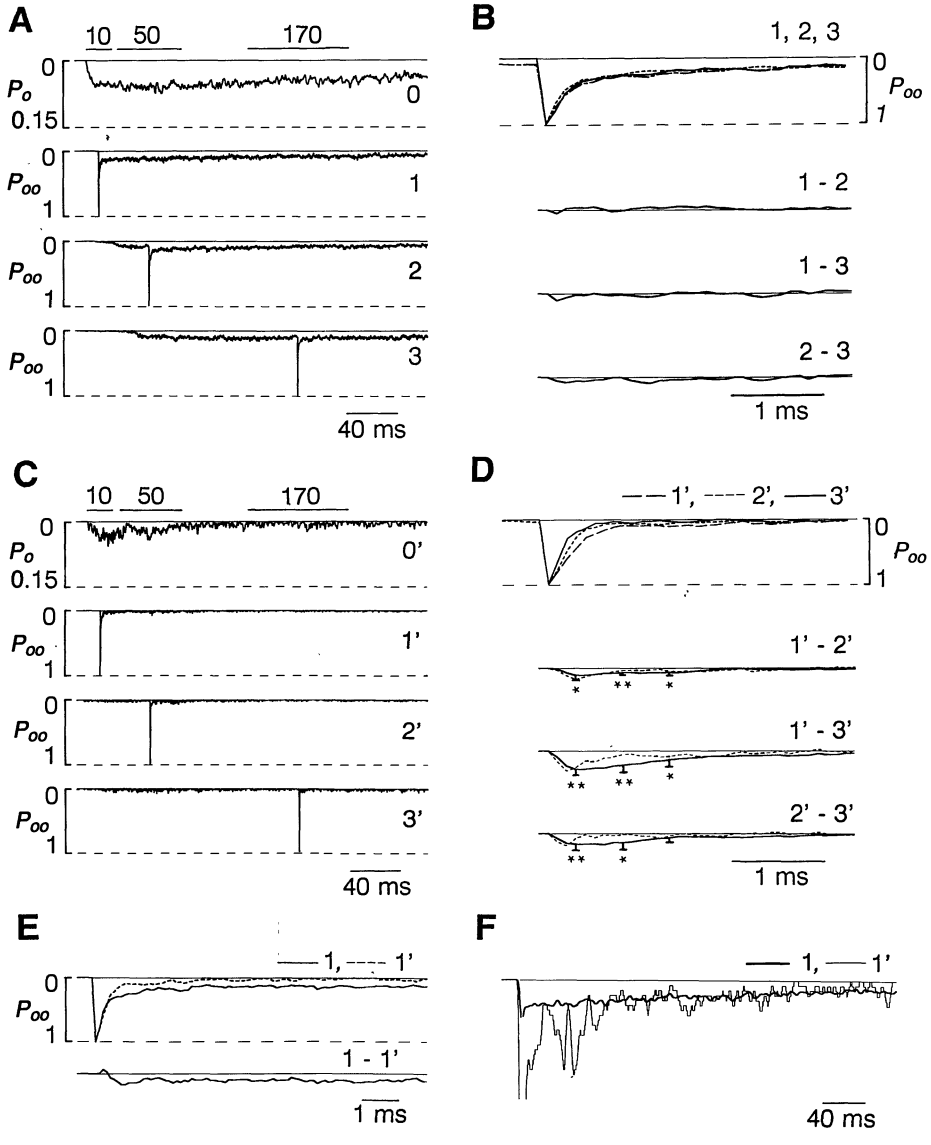

Fig. 2. Conditional open probability analysis with Ba^{2+} (A and B) and Ca^{2+} (C and D) as charge-carrier. Voltage steps to +20 mV throughout. (**A**) Trace 0 plots simple open probability, P_o, with horizontal bars above marking conditioning windows used to calculate conditional open probabilities. Traces 1 to 3 plot P_{oo}. P_o was low pass–filtered at 500 Hz. (Patch rle57.) (**B**) (Top) Superimposition of traces 1 to 3 (from A), after alignment at t_j and time base expansion. (Bottom) Difference traces of superimposed P_{oo}. (**C**) Identical format and conditioning windows as in (A), except with Ca^{2+} as charge carrier. (Patch rles64.1.) (**D**) Analogous format to (B). Lower three plots: Difference traces for P_{oo} curves 1′, 2′, and 3′ appear as dashed lines; mean difference traces from six patches plot the solid curve. Standard deviations are shown, along with significance levels by two-tailed, paired *t*-test [Double stars (**)], $P < 0.01$; single star (*), $P < 0.05$). (**E**) (Top) Comparison of P_{oo} conditioned on first openings with Ba^{2+} (trace 1) and with Ca^{2+} (trace 1′). (Bottom) Difference between traces 1 and 1′ above. (**F**) Comparison of decay of respective $P_{oo}(t, 10)$ with Ba^{2+} (trace 1) and Ca^{2+} (trace 1′). Traces were low pass–filtered at 100 Hz, and scaled in amplitude to facilitate comparison of slow decay phases.

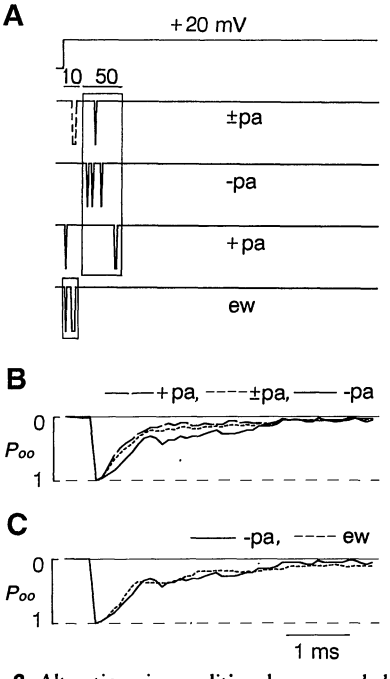

Fig. 3. Alterations in conditional open probabilities in response to different degrees of opening before instant of conditioning. (**A**) Schematic of various ways of calculating $P_{oo}(t, t_j)$. Voltage protocol and conditioning windows centered at 10 and 50 ms are displayed at top. Upper three traces illustrate different ways of calculating $P_{oo}(t, 50)$ according to activity before the conditioning window. Bottom trace summarizes how $P_{oo}(t, 10)$ is calculated; because the window at 10 ms extends to the beginning of the voltage step, conditioning occurs on first openings. (**B**) Superposition of various subtypes of $P_{oo}(t, 50)$. (**C**) Superimposition of −pa and ew, after alignment at t_j. (Patch r2es46, with Ca^{2+} as the charge-carrier.) Confirmatory results in a total of six patches.

with Fig. 2, but the mechanism of Ca^{2+}-facilitated inactivation requires the former to be true. We discriminated between these possibilities by considering three subtypes of $P_{oo}(t, t_j)$ (Fig. 3). Different sets of constraints can be imposed in the calculation of $P_{oo}(t, t_j)$, where t_j is 50 ms [$P_{oo}(t, 50)$] (Fig. 3A). In the usual method, each time an opening appears in the window at 50 ms, regardless of preceding activity, that record is included in the calculation of this sort of $P_{oo}(t, 50)$ [Fig. 3A, trace ± pa (prior activity)]. From Fig. 2, we know that this type of $P_{oo}(t, 50)$ will decay more quickly than $P_{oo}(t, 10)$ derived from a window at the start of the pulse [Fig. 3A trace ew (early window)]. The second and third traces illustrate alternate ways of calculcating $P_{oo}(t, 50)$: in addition to the requirement for openings within the window, we also specify that there must be preceding activity (trace +pa) or that there must not be preceding activity (trace −pa). If rate constants vary trivially with time spent at the activating potential, all three subtypes of $P_{oo}(t, 50)$ should decay with the same time course. In contradiction, the three subtypes of $P_{oo}(t, 50)$ demonstrate progressively faster decay rates as the history of openings is increased (decay rates: +pa > ±pa > −pa) (Fig. 3B). In fact, $P_{oo}(t, 50)$ without prior activity (−pa) virtually superimposes upon $P_{oo}(t, 50)$ (ew) in Fig. 3C, arguing that, without prior openings, gating properties of the channel are the same at 50 ms as they were at the beginning of the voltage step.

What characteristic of channel openings initiates the change in gating parameters? The mechanism of Ca^{2+}-facilitated inactivation holds that the decisive feature be Ca^{2+} entry into, or through, open channels (*4–8*). Figure 3 supports this view but is also consistent with a dependence on channel openings per se, with no requirement for Ca^{2+} entry. We addressed this uncertainty by examining the effects of voltage steps to the reversal potential (Fig. 4). The steps to +20 mV serve as the control (Fig. 4A); as expected from Fig. 2, $P_{oo}(t, 10)$ (trace 1) decays from unity more slowly than does $P_{oo}(t, 110)$ (trace 2). In Fig. 4B, we applied an 80-ms prepulse to +120 mV [≥ reversal potential (*18*)], where Ca^{2+} entry is diminutive (*19*) but P_o is large, as gauged by P_o after the prepulse (trace 0′). If Ca^{2+} entry is required to alter gating, then the decay of $P_{oo}(t, 110)$ (trace 2′), conditioned on first openings after the prepulse, should be like that derived from first openings of a pristine channel (Fig. 4A, trace 1). The crucial tests are shown in Fig. 4, C and D: after alignment at t_j, $P_{oo}(t, 110)$ following the prepulse (trace 2′) superimposes upon $P_{oo}(t, 10)$ (Fig. 4C, trace 1), but it declines more slowly than $P_{oo}(t, 110)$ with no prepulse (Fig. 4D, trace 2). Thus, gating rate constants vary with prior Ca^{2+} entry into, or through, open channels; openings per se are insufficient.

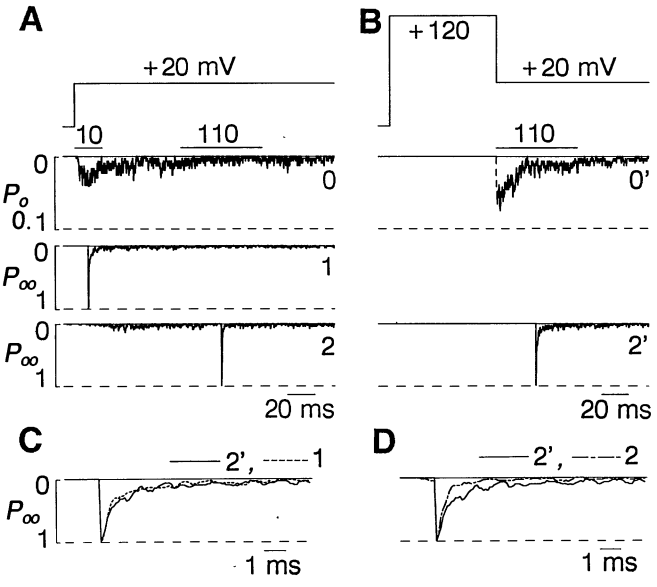

Fig. 4. No change in conditional open probabilities despite openings at the reversal potential. (**A**) (Top) Voltage protocol for direct steps to +20 mV from a holding potential of −45 mV. Trace 0: simple open probability, P_o, with horizontal bars above marking conditioning windows centered at 10 and 110 ms. The window at 10 ms extends to the beginning of the voltage step. Traces 1 and 2: $P_{oo}(t, t_j)$ derived from the conditioning windows in (A). (**B**) (Top) Voltage protocol with 80-ms prepulse to +120 mV; same holding potential. Trace 0′: P_o after prepulse, with horizontal bar above marking conditioning window centered at 110 ms [identical to that in (A)]. Because the window at 110 ms extends to the beginning of the period at +20 mV, conditioning occurs on first openings after the prepulse. Trace 2′: $P_{oo}(t, 110)$ based on window above trace 0′. No information is available during prepulse because unitary currents are virtually zero. (**C**) Superposition of traces 2′ and 1 after alignment at t_j. (**D**) Superposition of traces 2′ and 2 after time alignment at conditioning instant. In (A) and (B), voltage protocols were alternated at 1.5-s intervals in patch rles62.1b, with Ca^{2+} as charge-carrier. Confirmatory results in a total of three patches.

These observations raise several points about Ca^{2+}-channel gating. First, our results establish that inhomogeneous models characterize the gating of cardiac, L-type Ca^{2+} channels when Ca^{2+} carries charge. Paradigms associated with homogeneous processes, such as conceptualization of duration histograms as the sum of exponentials (*17*), cannot be entertained without modification.

Second, the chief effect of Ca^{2+} entry is not to speed inactivation to an absorbing state (*6*), but rather to favor occupancy of a closed state from which the channel can still reopen (*5*). Figure 2E shows $P_{oo}(t, 10)$ with Ba^{2+} and Ca^{2+} as charge-carrier (traces 1 and 1′); the main effect of Ca^{2+} is to depress the pedestal so that once a channel is open, it is much more likely to be subsequently closed. Nevertheless, because the smaller pedestal with Ca^{2+} is decidedly nonzero in the scaled-up plot of $P_{oo}(t, 10)$ (Fig. 2F, trace 1′), reopenings continue to occur for hundreds of milliseconds, thereby arguing against rapid inactivation to an absorbing state. In fact, the rate of absorbing inactivation, gauged by the decay of $P_{oo}(t, 10)$ toward zero (Fig. 2F), is slow and surprisingly similar with both Ba^{2+} and Ca^{2+} as charge-carriers (traces 1 and 1′, respectively, after normalization), suggesting that it may be strictly voltage-dependent. Facilitation of closed-state occupancy may be of physiological advantage: if $[Ca^{2+}]_i$ climbs and then plummets during an action potential, occupancy of a closed state could be reversibly increased. In contrast, enhancement of absorbing inactivation would preclude such reversible regulation.

Third, if Ca^{2+} does little to promote absorbing inactivation of the channel, what underlies the rapid decay of macroscopic Ca^{2+} currents? Fortunately, the genesis of macroscopic Ca^{2+} current [$I(t)$] can still be analyzed by the formalism of Aldrich and co-workers (*20*), despite inhomogeneous gating:

$$I(t) = N\, i\, [f(t) * P_{oo}(t, 0)]$$

where N is channel number, $f(t)$ is probability density of first openings, and * is the convolution operator. The expression still works because openings must occur before alterations in gating begin (Fig. 3), and $f(t)$ relates to first openings. With Ca^{2+}, $P_{oo}(t, 0)$ is short-lived (Fig. 2C, ~ trace 1′) relative to typical $f(t)$ (*15*), so that $I(t) \propto Nif(t)$; hence, the decay of macroscopic Ca^{2+} current parallels the diminution of first opening rate, $f(t)$ (*20*). In contrast, $P_{oo}(t, 0)$ is long-lived with Ba^{2+} (Fig. 2A, ~ trace 1), so that $I(t) \propto NiP_{oo}(t, 0)$; thus, decay of macroscopic Ba^{2+} current likely reflects absorbing inactivation (Fig. 2F).

Fourth, slow changes in $P_{oo}(t, t_j)$ that evolve over more than 100 ms (Figs. 2 and 4) rule out an exclusive role for mechanisms in which Ca^{2+} binding to the permeation pathway directly modifies gating (*21*). Al-

though analogous theories explain altered gating in K^+ channels (*22*), Ca^{2+} binding to the permeation pathway would equilibrate within microseconds of opening (*19*)–too fast to account for slow changes in $P_{oo}(t, t_j)$. A more plausible mechanism might be Ca^{2+} binding to an intracellular site outside the permeation pathway; diffusion (*23*) could then provide the requisite delays. Other possibilities include Ca^{2+} binding to an intrapore site with slow kinetics, or $[Ca^{2+}]_i$-mediated phosphorylation or dephosphorylation (*24*) of the channel or an associated G protein (*25*). In contrast, Ca^{2+} entry also confers some very rapid changes upon gating (Fig. 2E). Since $P_{oo}(t, t_j)$ for both charge-carriers here arises from first openings, comparison of the two traces indicates how quickly Ca^{2+} entry alters gating. The difference trace below shows that changes in gating produced by Ca^{2+} entry reach a quasi-equilibrium within 1 ms, arguing against an exclusive role for the slower mechanisms enumerated above. Diffusion constraints (*23*) suggest that Ca^{2+} inside or near the permeation pathway should be involved in this rapid effect. It will be important to establish whether a common mechanistic paradigm for Ca^{2+}-sensitive modulation of gating is shared among Ca^{2+}-channel relatives: L-type and, perhaps, N-type Ca^{2+} channels of vertebrate neurons are among the prime candidates.

REFERENCES AND NOTES

1. S. G. Rane, G. G. Holz, K. Dunlap, *Pfluegers Arch.* **409**, 361 (1987); D. Lipscombe, S. Kongsamut, R. W. Tsien, *Nature* **340**, 639 (1989).
2. T. Tanabe, A. Mikami, S. Numa, K. G. Beam, *ibid.* **344**, 451 (1990).
3. T. Tanabe, K. G. Beam, J. A. Powell, S. Numa, *ibid.* **336**, 134 (1988).
4. P. Brehm and R. Eckert, *Science* **202**, 1203 (1978); D. Tillotson, *Proc. Natl. Acad. Sci. U.S.A.* **76**, 1497 (1979).
5. R. Eckert and J. E. Chad, *Prog. Biophys. Mol. Biol.* **44**, 215 (1984).
6. K. S. Lee, E. Marban, R. W. Tsien, *J. Physiol. (London)* **364**, 395 (1985).
7. R. S. Kass and M. C. Sanguinetti, *J. Gen. Physiol.* **84**, 705 (1984).
8. M. Bechem and L. Pott, *Pfluegers Arch.* **404**, 10 (1985).
9. D. Lux and A. M. Brown, *Science* **225**, 432 (1984).
10. R. L. Rosenberg, P. Hess, R. W. Tsien, *J. Gen. Physiol.* **92**, 27 (1988).
11. Guinea pig ventricular myocytes were enzymatically isolated (*19*), and placed in 5 mM KCl, 20 mM potassium taurine, 120 mM potassium glutamate, 2 mM $MgCl_2$, 1 mM adenosine-5′-triphosphate (Ca salt), 2 mM EGTA, 10 mM Hepes-KOH, pH 7.4, at room temperature. The high K^+ concentration approximately zeroes the membrane potential, enabling estimates of transpatch potentials. 8-Bromocyclic AMP (0 to 1 mM) was included to increase activity. Pipettes contained 160 mM $BaCl_2$ or $CaCl_2$, as indicated, along with 10 mM Hepes-KOH, pH 7.4. Unitary currents were obtained in the cell-attached mode [O. P. Hamill, A. Marty, E. Neher, B. Sakmann, F. J. Sigworth, *Pfluegers Arch.* **391**, 85 (1981)], sampled at 10 kHz, and filtered at 2 kHz with Ba^{2+} as charge carrier, and at 0.65 to 1 kHz with Ca^{2+} as charge-carrier (−3 dB, 4-pole Bessel). Records, with leak and capacity currents eliminated by subtraction of smooth functions, were idealized by half-height criteria. These were used to construct ensemble averages and conditional open probabilities.
12. P. Kostyuk, N. Akaike, Y. Osipchuk, A. Savchenko, Y. A. Shuba, *Ann. N.Y. Acad. Sci.* **560**, 63 (1989).
13. R. W. Hadley and J. R. Hume, *J. Physiol. (London)* **389**, 205 (1987).
14. A. Cavalie, R. Ochi, D. Pelzer, W. Trautwein, *Pfluegers Arch.* **398**, 284 (1983).
15. F. J. Sigworth, *Biophys. J.* **34**, 111 (1981).
16. One-channel patches, as judged by absence of stacked openings, were used. Idealized records with openings during a conditioning window centered at t_j were shifted to align the first open point in the window at t_j. Time-shifted records were averaged and normalized by i to yield $P_{oo}(t, t_j)$. Distortion from noise and missed events should be independent of t_j. Thus, differences in $P_{oo}(t, t_j)$ are genuine, although the time course may be distorted by lower bandwidths required with Ca^{2+} as charge-carrier. With simple steps to +20 mV, the majority of active records showed mode 1 (Fig. 1A). A minority exhibited mode O_a and mode 2 [D. T. Yue, S. W. Herzig, E. Marban, *Proc. Natl. Acad. Sci. U.S.A.* **87**, 753 (1990)] and were excluded in P_{oo} analysis to ensure that a single open state predominated. After prepulses (as in Fig. 4), mode 2 was observed more frequently [D. Pietrobon and P. Hess, *Nature* **346**, 651 (1990)], but still in the minority of records.
17. D. Colquhoun and A. G. Hawkes, *Proc. R. Soc. Lond. Ser. B* **199**, 231 (1977).
18. P. Hess, J. B. Lansman, R. W. Tsien, *J. Gen. Physiol.* **88**, 293 (1986).
19. D. T. Yue and E. Marban, *ibid.* **95**, 911 (1990).
20. R. W. Aldrich, D. P. Corey, C. F. Stevens, *Nature* **306**, 436 (1983).
21. D. Swandulla and C. M. Armstrong, *Proc. Natl. Acad. Sci. U.S.A.* **86**, 1736 (1989).
22. C. M. Armstrong and J. Lopez-Barneo, *Science* **236**, 712 (1986); C. Miller, R. Latorre, I. Reisin, *J. Gen. Physiol.* **90**, 427 (1987); S. D. Demo and G. Yellen, *Biophys. J.* **57**, 15a (1990).
23. J. E. Chad and R. Eckert, *Biophys. J.* **45**, 993 (1984).
24. D. Armstrong and R. Eckert, *Proc. Natl. Acad. Sci. U.S.A.* **84**, 2518 (1987).
25. R. H. Scott and A. C. Dolphin, *Nature* **330**, 760 (1987).

26. We thank K. Y. Yau and K. J. Gingrich for valuable comments. Supported by the USPHS (grant R29-HL43307 to D.T.Y. and grant 5-T32-GM07057 to J.P.I.), the American Heart Association (Established Investigatorship to D.T.Y.), and the Medical Research Council of Canada (P.H.B.).

22 June 1990; accepted 12 September 1990

A New Arbovirus from *Aedes albopictus*, an Asian Mosquito Established in the United States

D. B. FRANCY, N. KARABATSOS, D. M. WESSON, C. G. MOORE, JR., J. S. LAZUICK, M. L. NIEBYLSKI, T. F. TSAI, G. B. CRAIG, JR.

Ten strains of a new arbovirus belonging to the Bunyamwera group (Bunyaviridae) were recovered from field-collected *Aedes albopictus* mosquitoes in Potosi, Missouri. This evidence indicates that this species may serve as an arbovirus vector in the United States. The urban-suburban distribution, aggressive biting behavior, and broad viral susceptibility of *Ae. albopictus* may lead to the transmission of viruses of known public health importance and perhaps of viruses hitherto not transmitted to humans because of the feeding pattern of their usual vectors.

AEDES ALBOPICTUS, A MOSQUITO SPECIES native to Asia, was discovered in Houston, Texas, in 1985 (*1*). It has now been found in 160 counties in 18 states. This species has previously been found in used tires entering the United States from Asian ports (*2*). Importation of used tire casings to the United States from Asia, primarily Japan, is a major business (*3*). It was therefore hypothesized that *Ae. albopictus* had come to the United States in used tire casings. This mode of introduction was confirmed in 1986 when larvae of *Ae. albopictus* were found in water-containing tires arriving at the port of Seattle from Tokyo (*4*).

Public health officials are concerned about the establishment of this species in the United States because it is a documented vector of dengue viruses in Asia (*5*). This species has also been shown experimentally to be a vector for a number of arboviruses (*6*); thus it could also become a vector of one or more of the indigenous U.S. arboviruses.

Aedes albopictus is an efficient laboratory vector of La Crosse (LAC) virus (*7*), and vertical transmission of LAC in *Ae. albopictus* has been shown (*8*). LAC virus is endemic in the Great Lakes region and produces encephalitis primarily in children under 15 (*9*). The vector of LAC virus is *Ae. triseriatus*, a mosquito which develops primarily in deciduous tree holes but which readily utilizes water-holding man-made containers as a larval habitat. Increased risk of human LAC encephalitis cases is associated with *Ae. triseriatus* development in man-made containers in and near the premises of case households (*10*) and with the numbers of potential water-holding containers on case premises (*11*). The fact that *Ae. albopictus* and *Ae. triseriatus* use similar larval habitats,

D. B. Francy, N. Karabatsos, C. G. Moore, Jr., J. S. Lazuick, T. F. Tsai, Division of Vector-Borne Infectious Diseases, Center for Infectious Diseases, Centers for Disease Control, U.S. Public Health Service, Fort Collins, CO 80522.
D. M. Wesson, M. L. Niebylski, G. B. Craig, Jr., Department of Biological Sciences, University of Notre Dame, Notre Dame, IN 46556.